Density functional simulations of silicon-containing point defects in diamond

J. P. Goss, P. R. Briddon, and M. J. Shaw
School of Natural Sciences, University of Newcastle upon Tyne, Newcastle upon Tyne NE1 7RU, United Kingdom
(Received 16 March 2007; revised manuscript received 13 June 2007; published 8 August 2007)

Silicon impurities in diamond lead to the appearance of the well known system of 12 lines around 1.681 eV, thought to arise from the silicon-vacancy complex. This system is produced by various treatments suggestive of other silicon-related centers in the material. In order to elucidate possible structures of Si in diamond, we have performed first-principles calculations. We show that interstitial Si is unstable at growth temperatures, substitutional Si is most likely visible only by vibrational mode spectroscopy, and complexes of silicon with lattice vacancies are electrically, paramagnetically, and optically active. In addition, we report on Si-N and Si-H complexes in the context of doping and the KUL3 electron paramagnetic resonance center, respectively.

DOI: 10.1103/PhysRevB.76.075204 PACS number(s): 61.72.Bb, 61.72.Ww, 71.20.Mq, 71.23.An

I. INTRODUCTION

Silicon is a common contaminant in chemical vapor deposited (CVD) diamond. The origin is typically environmental, being etched from the deposition chamber or substrate[1] but may be deliberately added during growth or by implantation. The clearest evidence for the presence of silicon defects comes from a system of 12 emission lines around 1.681 eV (737nm), corresponding to three silicon isotopes and orbitally degenerate ground and excited states.[2] The defect is extremely stable, surviving annealing temperatures exceeding 2000 °C,[2] and has been proposed as a single photon source.[3]

The emission intensity increases subsequent to electron irradiation and annealing to temperatures where the vacancy is mobile, suggesting that the optical center involves both Si and vacancies.[2,4,5] This also implies that Si is present in other forms (structures and/or charge states) in as-grown material.

Other optical transitions lie close in energy to the 12-line system, leading to some difficulty in identifying a unique source of optical activity. The peak position of the silicon-related center is variously quoted in the 1.681–1.685 eV range. The GR1 peak, associated with the neutral vacancy,[6] lies at 1.673 eV and an optical absorption arising from the self-interstitial lies at 1.685 eV.[7,8] Another absorption center at 1.640 eV has also been assigned to a silicon-related defect.[9] Hence, rather than use an emission energy, we refer to the silicon-related 12-line system as "TLS."

Many properties of the TLS have been determined. Higher concentrations are observed with higher annealing temperatures[10,11] and there is a similar broad correlation with substitutional nitrogen concentration.[12] However, there is also evidence that nitrogen suppresses the formation of the optical center,[13] and a maximum in intensity with nitrogen in the growth gas is observed.[14] In high-temperature, high-pressure (HPHT) synthesized diamond the formation of optically active Si appears to be suppressed rather than enhanced by the uptake of nitrogen,[15] although the uptake of Si in HPHT material is much lower than in CVD diamond. Oxygen also appears to suppress the uptake of silicon in CVD growth.[16]

In addition, the TLS is distributed highly inhomogeneously,[17,18] has a very short radiative lifetime ($\sim$1–4 ns),[19,20] is associated with a vibrational mode[21] at 515 cm^{-1}, and uniaxial stress measurements indicate either a D_2 or C_2 symmetry.[22] The proximity of the vibrational mode to the Raman frequency of bulk silicon has been used as an argument to assign this system to one containing a Si-Si bond.[21,23] However, the spectral location of a vibrational mode is certainly not unambiguous in such an assignment, and we shall show here that such a mode may be obtained without the need for two silicon impurities.

The TLS is also seen in absorption.[24,25] There are other absorption centers close in energy which are not seen in emission. These additional centers are less stable than the TLS, giving rise to an apparent "dip" in luminescence intensity with annealing temperature, which does not reflect a change in concentration.[24]

The TLS is a molecular rather than excitonic transition,[26] implying the presence of multiple gap states. This is consistent with distinct charge states and a role for N in the formation of the TLS relating to the electron chemical potential μ_e. Experimental estimates for electrical transitions for the TLS are $E_c-2.23$ eV (Ref. 26) and $E_c-2.05$ eV.[27]

Finally, there are also assignments of silicon-related centers in electron paramagnetic resonance (EPR). The KUL1 ($S=1$) and KUL8 ($S=1/2$) centers are reputedly different charge states of the same defect, with the former having trigonal symmetry and the latter containing one more electron than the former.[9,27–29] KUL3 may contain both Si and hydrogen.[30] Like the TLS, KUL1 is very stable, surviving an annealing temperature of 1400 °C.[28] However, there is no apparent correlation between the EPR and optical centers.[9]

Relatively little computational work has been performed on silicon in diamond. Small atomic clusters were used to simulate substitutional (Si_s) and interstitial (Si_i) silicon species, the latter forming split-interstitial structures, where a Si-C pair share a single lattice site.[31] However, the methodology and size of the cluster place the results in some doubt. For example, the Si-C bond length for Si_s relaxed to 1.86 Å, around 8% longer than the bond lengths calculated using density functional techniques in much larger periodic simulation cells.[32] Later cluster calculations indicated that a nonbonded interstitial and split-interstitials were at best metastable relative to the formation of a self-interstitial and insertion of Si into the lattice.[33]

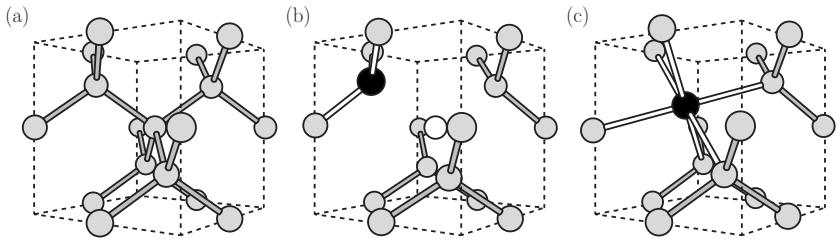

FIG. 1. Schematics of Si_s-V in diamond. The black and gray atoms represent Si and C, respectively, with the white circle in (b) indicating the vacancy. (a) shows a section of defect-free diamond, (b) shows the same section with Si on a substitutional site neighboring V, and (c) shows the split-vacancy configuration.

Si_s is isoelectronic with the host. One study suggested a strain-related level in the band gap,[34] and other calculations show that it is stable only in the neutral charge state.[32] Si_s dilates the lattice,[32,35] with theory suggesting that each Si_s displaces the volume of 1.6 host atoms.

Greater focus has been placed in modeling complexes of silicon with a lattice vacancy. It was previously shown that the electronic structure of the negative charge state of a complex made up from Si_s and a lattice vacancy (V) is consistent with many of the properties of the TLS.[36]

Si_s-V, rather than consisting of Si_s adjacent to V, theoretically has a split-vacancy structure. Both configurations are illustrated in Fig. 1. Si_s-V has two doubly degenerate states in the band gap, so that $(Si_s\text{-}V)^0$ has an $e_u^4 e_g^2$ ground-state configuration, most probably in the $^3A_{2g}$ multiplet.[36] In the negative charge state, orbitally degenerate ground- and excited-state multiplets may be obtained from the configurations $e_u^4 e_g^3$ and $e_u^3 e_g^4$, respectively, consistent with the TLS observations.[2] We note that these ^2E_g and ^2E_u multiplets are Jahn-Teller systems.

Calculations show that Si_s-V has donor and acceptor levels, the former lying 0.3–0.6 eV above E_v and the latter around $E_v+1.5$ eV.[32,37]

More recently, intermediate neglect of differential overlap calculations suggest that the neutral charge state has a propensity for the Si atom to move toward three of the six neighbors.[38] The splittings in the TLS are then interpreted as the tunneling between the two equivalent C_{3v} structures of the $S=1$, neutral configuration.

Finally, modeling suggests that codoping diamond with Si and N may yield n-type material via the formation of Si_4N complexes.[34] However, the efficacy of this complex as a dopant is disputed.[39,40]

In order to place suggestions in the literature on a firmer theoretical basis, we present the results of first-principles, density functional based calculations on the likely structure and properties of a range of states of silicon in diamond. Where possible, we relate the calculations to the observations.

II. METHOD

Calculations were carried out using the local-spin density functional technique, implemented in AIMPRO (Ref. 41) (*ab initio* modeling program). To simulate defects, mostly 64- and 216-atom, cubic supercells of side length $2a_0$ or $3a_0$ have been used. The Brillouin zone is sampled using the Monkhorst-Pack scheme,[42] generally with $2\times2\times2$ special k points. Core electrons are eliminated by using norm-conserving pseudopotentials.[43]

The wave-function basis sets for all atoms are based on independent s and p Gaussians[44] with four widths. For carbon, one further set of d Gaussians was included to account for polarization, whereas for Si and N, two and four sets of d Gaussians were added. Three sets of s and p Gaussians were centered on each H atom.

The charge density is Fourier transformed using plane waves with a cutoff of 300 Ry, yielding total energies converged to ~1 meV. The lattice constant and bulk modulus are within ~1 and 5%, respectively of experimental values, while the direct and indirect band gaps at 5.68 and 4.26 eV, respectively, are close to previously published plane-wave values.[45]

Diffusion barriers have been obtained by using the climbing nudged elastic band (NEB) formalism.[46,47]

The formation energy of X in charge state q is calculated using[48]

$$E^f(X,q) = E(X,q) - \sum \mu_i + q(E_v^X + \mu_e) + \chi(X,q), \quad (1)$$

where E is the total energy, μ_i and μ_e are the chemical potentials of the atoms and electrons, respectively, E_v^X is the energy of E_v in the defect cell, and χ is the correction for periodic boundary conditions, for which we include only the Madelung term.[49] For cubic supercells of side lengths $2a_0$ and $3a_0$, this is around $0.53q^2$ and $0.35q^2$ eV, respectively. The form of the correction due to periodic boundary conditions is controversial,[50–55] and one must take care in applying any *post hoc* term to the total energy. By convention, we define a binding energy by $E^b(XY)=E^f(X)+E^f(Y)-E^f(XY)$.

Hyperfine interactions are modeled as outlined previously.[56] Briefly, this involves the combination of pseudopotentials and reconstructed all-electron wave functions in the core region.[57,58] Reconstruction of the ion cores allows us to calculate the hyperfine tensor elements within a frozen-core all-electron wave-function approximation, without the computational difficulties associated with a full all-electron calculation. Generally, for well characterized defects, agreement between calculated values and experiment is better when using a functional with the generalized gradient approximation, and all calculated hyperfine tensors within this paper are obtained using the formulation of Perdew *et*

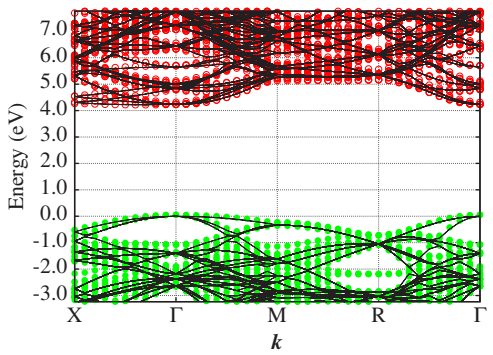

FIG. 2. (Color online) Kohn-Sham bands in the vicinity of the band gap along high-symmetry directions of the first Brillouin zone of a 216-atom supercell containing Si_s. The green, filled circles show occupied levels, and red, empty circles show empty bands. The black lines are defect-free bands. The zero of energy is defined as the valence band top of diamond.

al.[59] For other aspects, the choice of functional has a relatively minor effect. For example, relative to the local density approximation values, the donor and acceptor levels of Si_s-V complexes, as well as the binding energy of a Si_s-N_s complex, all differ by less than 0.1 eV.

Finally, vibrational modes are obtained by diagonalization of the dynamical matrix using second derivatives of energy with respect to atomic displacements for all atoms calculated using a finite difference approach.

III. RESULTS

A. Substitutional Si

We begin with substitutional silicon. The relaxed Si-C bonds are 1.71 Å, 12% longer than host bonds but 9% smaller than those of cubic SiC. The Si_s band structure, plotted in Fig. 2, shows that the strain has little impact in the vicinity of the band gap, consistent with the previously reported electrical inertness[32] but perhaps at variance with other suggestions.[34]

More interesting are the vibrational properties of this center. The strain immediately surrounding Si_s leads to several T_2 modes in the vicinity of the one-phonon maximum that have a substantial component on the four carbon neighbors. For example, one mode around 1333 cm^{-1} is relatively localized but has very little amplitude upon the Si atom, as shown in Fig. 3. We note that in addition to the high-frequency modes, there is a T_2 mode calculated at 430 cm^{-1} localized partly on the Si atom. This is a region of low bulk density of states. The silicon isotopic shift with ^{29}Si is around 3 cm^{-1}, with a similar further shift for ^{30}Si, as shown in Fig. 3(c). Although precise frequencies are not possible using the current approach, infrared-active modes around the one-phonon maximum and at lower frequency may hold the key to direct identification of Si_s, since Si_s is theoretically invisible to electronic-optical spectroscopy, magnetic resonance, and electrical characterization.

In line with this assertion, we note that in intentionally Si doped CVD diamond, there is a vibrational mode detected at

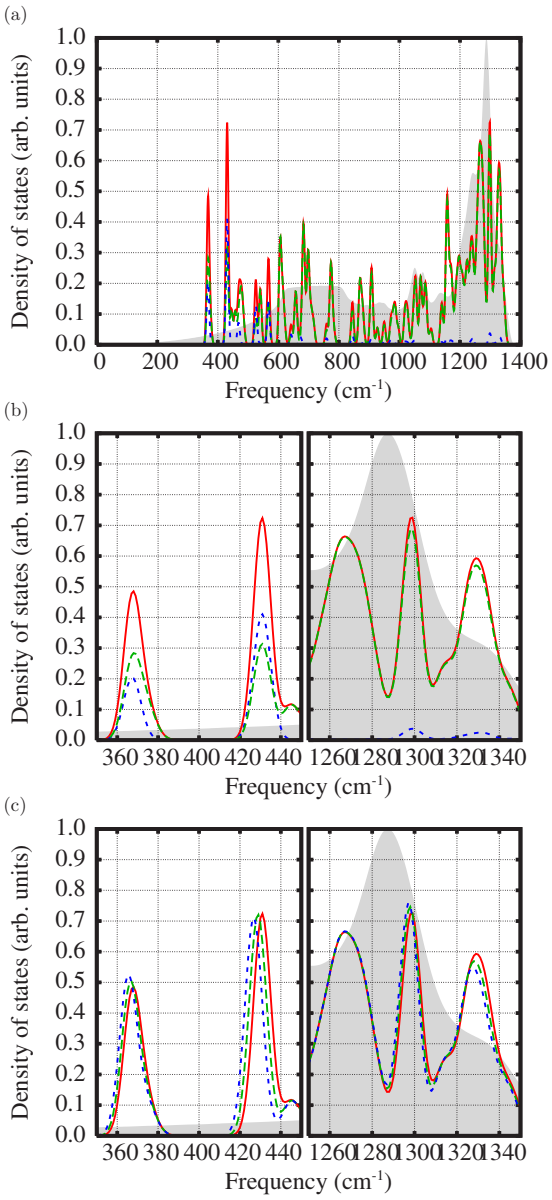

FIG. 3. (Color online) Vibrational partial density of states for Si_s in diamond taken from the spectrum at the zone center using the 216-atom supercell. (a) shows the full range of frequencies with the red, solid line indicating the partial density of states on the Si atom and its four C neighbors, which is then divided into contributions from the Si (blue, dotted line) and C atoms (green, dashed line). (b) shows two frequency ranges of interest with the line styles and colors following those in (a). (c) shows the reduced frequency ranges with the solid (red), dashed (green), and dotted (blue) lines indicating ^{28}Si, ^{29}Si, and ^{30}Si, respectively. In all cases, the gray areas show the calculated bulk phonon density of states.

around 1338 cm^{-1}.[60] If this mode is to be correlated with Si_s, according to our current calculations, this must be dominated by the motion of the surrounding carbon atoms and will show relatively little difference upon isotopic substitution for the silicon atom, as shown in Fig. 3(c).

Finally, we note that previous calculations suggest that Si_s displaces a relatively large volume.[32,35] Each Si atom that replaces a carbon host displaces 1.6 times the volume per

host atom. This means that in a material with relatively high concentration of Si_s, one might anticipate an increase in the lattice constant. The fractional change in lattice constant is around $\Delta V/3 \times [Si_s]$, where ΔV is the displaced volume and $[Si_s]$ is the fractional concentration of Si_s relative to the carbon host.[61] Then, for a Si_s concentration of 200 ppm, there is 0.01% increase in a_0.

B. Aggregated substitutional Si

We find multiple Si_s centers high in energy due to elastic repulsion. Nearest-neighbor Si_s pairs are unbound by 3.0 eV, with second-neighbor pairs bound by just 0.2 eV, of the order of the error bar of the method. The strain, in contrast to isolated Si_s, *does* push occupied levels into the band gap, but the effect is modest and diminishes with increasing Si-Si separation.

The most likely route to observing pairs from experiment, as with Si_s, is vibrational mode spectroscopy. For the nearest-neighbor D_{3d} pair, there is an A_{2u} vibrational mode at around 314 cm^{-1}, localized on the two impurities and their immediate neighbors. This shifts to lower frequency by 2 cm^{-1} for each ^{29}Si and 4 cm^{-1} for each ^{30}Si and consists of motion of the Si pair along the Si–Si bond direction. A second mode around 900 cm^{-1}, representing an A_{1g} bond stretch between the Si atoms, shifts by around 4 and 7 cm^{-1} upon substitution by one or two ^{29}Si. The substantial upward shift in frequency relative to the Raman frequency of bulk silicon is a result of the much shorter Si–Si bond in this defect, at just 83% of the bulk silicon value. In addition, there are C-related E modes around 400 cm^{-1} and the one-phonon maximum which shifts only slightly with Si isotope.

The second-neighbor pair has a more weakly localized, IR-active mode around 410 cm^{-1} which shifts with Si isotope, as well as IR-active modes around 600 and 1200 cm^{-1} and the one-phonon maximum localized more on the common C neighbor than the Si atom.

Larger aggregates that we examined are also weakly bound or unbound, and although pairs would theoretically be identifiable from IR-active modes, we conclude that Si_s exhibits no propensity to cluster, and are, therefore, of only very limited interest.

C. Nitrogen-silicon substitutional complexes

Since there is a relationship between silicon and nitrogen for the TLS and due to the suggested n-type Si-N codoping,[34] we have investigated the nature of complexes made up from these constituents.

Despite Si_s and N_s compressing their surroundings,[32] Si_s-N_s is bound by 1.2 eV as a nearest-neighbor pair, with a deep donor level, degenerate with isolated N_s to within the computational error.

Our calculations for Si_4N have already been reported for large supercells.[40] Here, we report on the intermediate complexes, $(Si_s)_n$–N_s, $n=2$ and 3. In analogy with Si_4N, the lowest energy configurations involve N_s with two or three Si_s neighbors, and as with Si_s-N_s, both complexes lead to deep donor levels close to that of isolated N_s.

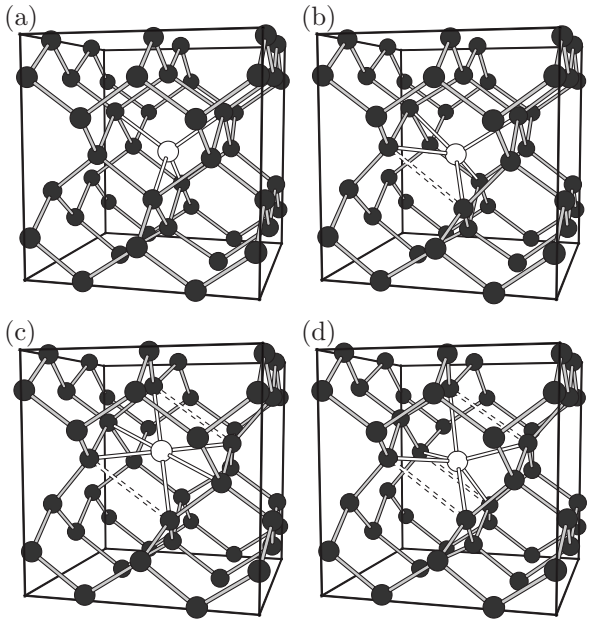

FIG. 4. Schematic structures of Si_i in diamond. (a) on site and (b) one, (c) two, and (d) three broken C-C bonds. The gray and white atoms are C and Si, respectively. The dashed and white "bonds" indicate broken host bonds and atoms within 1.8 Å of Si, respectively.

$(Si_s)_n$-N_s is bound relative to $(Si_s)_{n-1}$-N_s and Si_s by around 1.2, 1.0, 1.1, and 0.5 eV for $n=1-4$. Our total binding energy of Si_4N is 3.7 eV, slightly higher than the initial value of 3.17 eV.[34] We reflect further upon the likelihood of forming Si-N complexes in Sec. IV.

D. Interstitial Si

The stability of silicon as an interstitial impurity has been re-examined. We relaxed on-site tetrahedral interstitial and then perturbed the geometry and rerelaxed with no symmetry constraint. Other than for $q=+4e$, the T-site structure is unstable, with the relaxation increasing for increasingly negative charge states.

There are four classes of relaxed geometry: (1) on-site interstitial stable only for $q=+4e$ [Fig. 4(a)], (2) a distorted T site where a single neighboring C-C bond is broken ($q=+3e$ and $+2e$) [Fig. 4(b)], (3) a distorted H site with two broken C-C bonds ($q=+1e$ and 0) [Fig. 4(c)], and (4) an approximately trigonal structure with three broken C-C bonds ($q=-1e$ to $-4e$) [Fig. 4(d)]. The breaking of C-C bonds relate to trapping of electrons, as recently found for interstitial Li and Na.[62] We also relaxed Si_i as a [001]-oriented split-interstitial pair but found it to be 1.6 eV higher in energy than that shown in Fig. 4(c). This is most likely due to the fact that silicon does not readily adopt an sp^2 hybridization.

The formation energy of the neutral charge state in equilibrium with silicon and diamond is 19.2 eV, and the charge dependence suggests that this is preferred for most values of μ_e, with a donor level at $E_v+1.0$ eV and an acceptor level at $E_c-0.5$ eV.

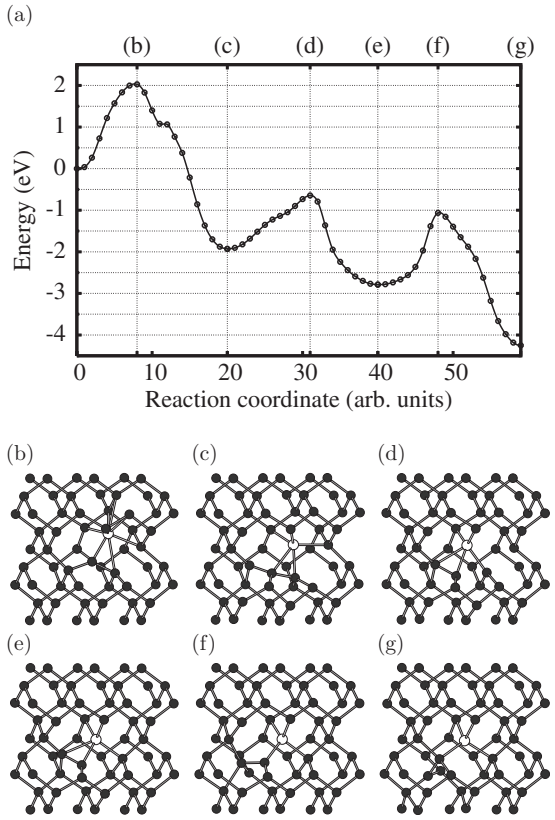

FIG. 5. (a) NEB barrier for the insertion of Si_i into the diamond lattice. Each point represents a NEB image, and the line is a guide to the eyes. Labels (b)–(g) relate points on the profile to schematics of intermediate and saddle point structures. Structures are colored as in Fig. 4. The initial Si_i structure, from which the zero of energy is defined, is shown in Fig. 4(c).

In order to assess the stability of Si_i, we have calculated the activation energy for the exchange of Si with a host atom, for which we find a relatively low energy barrier. Figure 5 shows the energy profile for three steps originating from that shown in Fig. 4(c). (c) is a distorted split-interstitial structure, (e) is Si_s immediately neighboring a self-interstitial, and (g) has a self-interstitial at a site removed from Si_s. The rate-limiting step is around 2 eV, so this process will readily occur at the growth temperature or during annealing following implantation. We conclude that an as-grown or implanted and annealed material will not retain a significant concentration of metastable, interstitial silicon.

E. Vacancy-silicon complexes

We first revisit Si_s-V to report calculated properties that complement those previously published.[32,36]

As indicated in the Introduction, the highest occupied level is doubly degenerate and half filled in the neutral charge state. This admits the possibility of adding and removing a number of electrons depending on the location of μ_e. The charge-dependent formation energy yields three electrical levels: a donor level at or just above E_v, an acceptor level around $E_v+1.5$ eV, and a *second* acceptor level around $E_c-2.1$ eV. The precise location of the electrical levels depends on the supercell size due in part to the term χ in E^f. However, the location of the level varies by just 0.1 eV across the 64- and 216-atom cubic supercells and a 256-atom bcc supercell, and we conclude that the second acceptor level coincides reasonably well with the experimental electrical transition of the TLS.[26,27]

We have also calculated the vibrational modes of the defect in three optically active charge states. There are no high-frequency vibrations but several lie in the 300–500 cm^{-1} range, as listed in Table I. In particular, although the calculated values are relatively low in frequency, there are vibrations broadly consistent with the 515 cm^{-1} mode of the TLS.

In addition, Table I lists the calculated hyperfine tensors for Si and neighboring carbon atoms. We note that in all charge states, the hyperfine interactions on the silicon atom are dominated by the isotropic component. This may be related to the published data for KUL1,[28] which has one interpretation including a Si atom with a nearly isotropic hyperfine tensor with two components of 79 MHz and one of 76 MHz. Although this agrees rather well with the calculated values for Si_s-V, there is some difficulty in assigning KUL1 to Si-V that the measurements do not suggest six equivalent carbon sites but a single site and a pair. The latter has associated hyperfine tensors with components of 29 and 42 MHz, which are in reasonable agreement with those calculated for the nearest neighbors, and the former has a much larger component of 140 MHz and two of 60 MHz. One possible explanation might be a distortion at the $S=1$ center akin to that

TABLE I. Calculated vibrational modes (cm^{-1}) and hyperfine tensors (MHz) for Si_s-V oriented along [111] in diamond. The irreducible representations of the modes within the D_{3d} point group are shown in parentheses. Δ_1 and Δ_2 indicate the downward shift in frequency with substitution of ^{29}Si and ^{30}Si, respectively. $A_\parallel$ and $A_\perp$ are ^{29}Si hyperfine components parallel and perpendicular to [111], respectively. A_1, A_2, and A_3 are hyperfine components lying along $[\bar{1}\bar{1}1]$, $[1\bar{1}0]$, and $[11\bar{2}]$, respectively, for ^{13}C at one of the neighboring sites. The angle in parentheses indicates the deviation of A_1 from $[\bar{1}\bar{1}1]$.

				^{29}Si		^{13}C		
	$^{28}Si_s$	Δ_1	Δ_2	$A_\parallel$	$A_\perp$	A_1	A_2	A_3
$(Si_s\text{-}V)^-$	455(E_u), 346(A_{2u})	5, 5	10, 9	74	78	61 (1°)	22	22
$(Si_s\text{-}V)^0$	466(E_u), 302(A_{2u})	7, 5	14, 10	78	82	51 (2°)	12	12
$(Si_s\text{-}V)^+$	414(E_u), 244(A_{2u})	6, 5	12, 8	87	91	56 (2°)	15	15

seen for the neutral divacancy.[63,64] Such a complex distortion may not be resolved in the calculations but is unlikely to lead to a single C site. Indeed, given the trigonal symmetry of KUL1,[30] it is difficult to construct any system that may have both unique and paired sites. Since a unique site must lie on the C_3 axis, the pairs cannot be linked by inversion symmetry. We conclude that no unambiguous assignment may be made on the basis of the currently available data.

We have also examined the suggestion that the energy is lowered for a displacement of Si along [111] toward three carbon atoms in the neutral, $S=1$ configuration.[38] We displaced Si a range of distances along the trigonal axis and allowed the neighboring carbon atoms to relax. No energy reduction was found.

For the positive and negative charge states, the D_{3d} structure yields many-body wave functions with ^2E_g symmetry. Both systems are subject to a Jahn-Teller distortion. In the absence of spin-orbit effects, this cannot be a displacement along [111] as such a displacement does not raise the orbital degeneracy. However, displacement of Si along, say, $[11\bar{2}]$ or $[1\bar{1}0]$ *would* split the e_g level. The latter generates a structure with C_2 symmetry, consistent with the uniaxial stress data for the TLS.[22,65] More likely, perhaps, is a distortion involving the neighboring carbon atoms, since the partially occupied bands are mostly localized on these atoms. For such distortions to lead to meV splittings, it seems likely that the energies and geometric changes involved are small, and we have been unable to obtain a stable distorted structure.

Previously,[32] the binding energy of the Si_s-V complex was determined to be 4.1 eV. Assuming Si_s-V does not diffuse, it would be lost by dissociation, the *barrier* to which would be 6.4 eV. Here, 2.3 eV of this energy corresponds to migration energy of the vacancy.[66] Such a high barrier is entirely consistent with the very high temperatures to which the TLS is stable.

An alternative path for loss of Si_s-V involves trapping additional vacancies, so we also examined Si_s-V_2. This may also be an important product in an implanted and annealed material. Using $E^f(V)=6$ eV,[67] the reaction Si_s-$V+V \rightarrow Si_s$-V_2 releases 2.9 eV. Thus, although Si_s traps a second V less efficiently than the first, such complexes with an estimated dissociation energy of 5.2 eV would also be stable at high temperatures.

Si_s-V_2 resembles Si_s-V in Fig. 1(c) with one of the six carbon neighbors removed (Fig. 6). The abundance of dangling bonds leads to several gap states, as plotted in Fig. 7, and the charge-dependent formation energy suggests that Si_s-V_2 has at least one acceptor level in the bottom half of the band gap. In addition, the combination of low symmetry with occupied and empty gap states lends the complex to optical activity, and although crude, the Kohn-Sham band structure indicates a transition energy in the 1.0–1.5 eV range and another close to the band-gap energy.

In the negative charge state, likely to occur in materials containing N_s, Si_s-V_2 would be an $S=1/2$ EPR center. For comparison with the values obtained for Si_s-V, we have also calculated the hyperfine tensor for Si_s-V_2. The unpaired electron is largely localized on the three carbon dangling bonds, as shown in Fig. 6. For ^{13}C in the site in the mirror plane but most distant from Si, $A_\parallel$ lies close to [111] with a magnitude of 307 MHz and $A_\perp=99$ MHz. The two remaining C dangling bond sites yield $A_\parallel=68$ MHz close to $[\bar{1}11]$ and $A_\perp=35$ MHz. In contrast, a ^{29}Si hyperfine interaction has an isotropic component of −43 MHz and a very small anisotropic term (<2 MHz). The hyperfine tensors on the other close-by C sites are all very small.

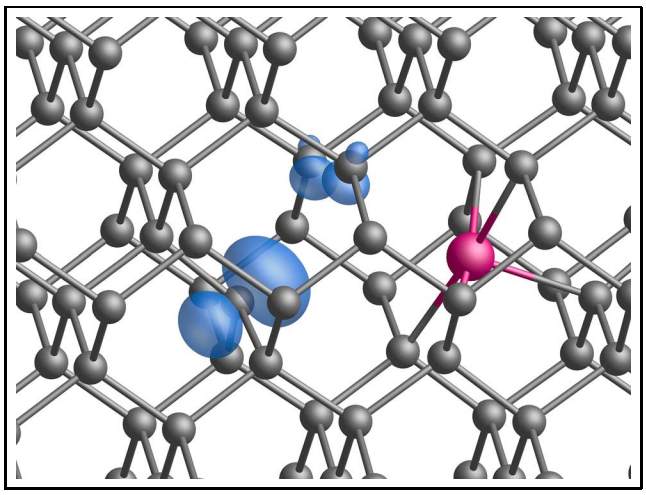

FIG. 6. (Color online) Schematic of the unpaired Kohn-Sham function for Si_s-V_2. The large, fivefold coordinated (pink) atom is Si and the remaining atoms are the carbon host. The isosurface is of the surface of constant spin density showing the localized nature of the orbital. The horizontal and vertical alignments are [110] and [001], respectively.

We showed in Sec. III B that aggregates of Si_s are energetically unfavorable. However, in the presence of a lattice vacancy, this is not the case. For $1<n\leq 4$, $(Si_s)_n$-V resemble V neighbored by Si_s rather than adopting split-vacancy structures. They are bound relative to their constituents by 6.1, 7.1, and 7.3 eV for $n=1$, 2, and 3, respectively. Since these exceed $E^f(V)$, they would form under equilibrium conditions in preference to Si_s, although this requires simultaneous incorporation of multiple silicon atoms or mobile species, both of which seem doubtful. Despite the large total binding energies, the incremental binding energy when adding consecu-

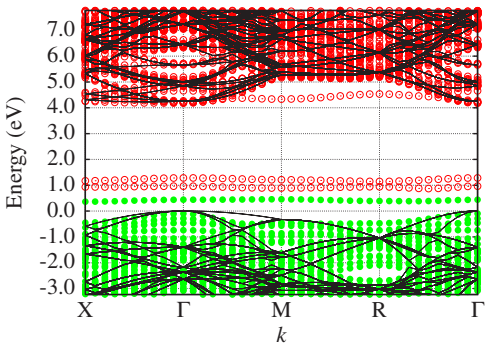

FIG. 7. (Color online) Band structure in the vicinity of the band gap along the high-symmetry direction of the first Brillouin zone of a 216-atom supercell containing Si_s-V_2. The symbols, lines, and axes are as described in Fig. 2.

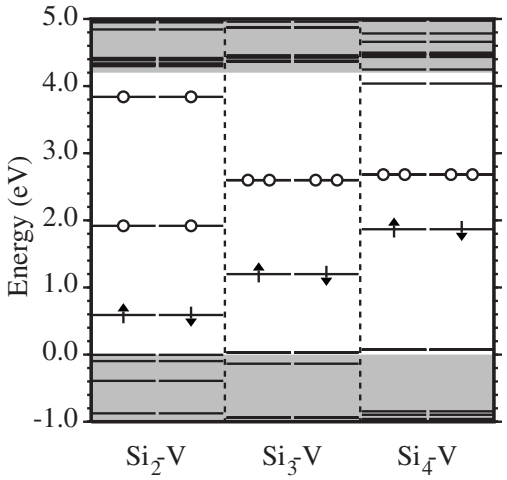

FIG. 8. Kohn-Sham eigenvalues at the Brillouin-zone boundary for $(Si_s)_n$-V, $n=2$, 3, and 4. The arrows indicate electron occupation and spin and circles show empty levels. The zero of energy is set to the bulk diamond valence band top and the shaded areas indicate bulk bands.

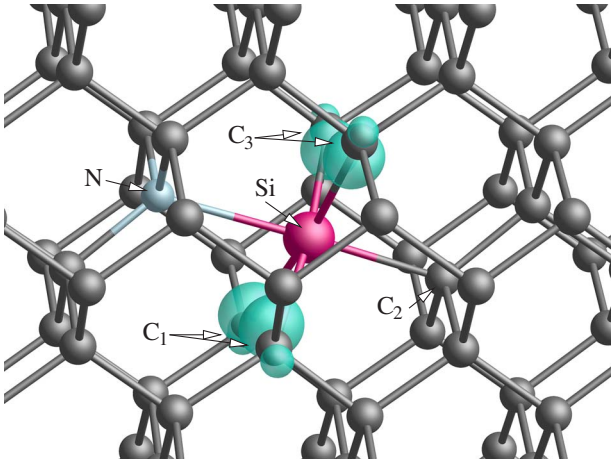

FIG. 9. (Color online) Schematic of the unpaired Kohn-Sham function for Si_s-V-N_s. Impurity atoms are as labeled, with all the remaining atoms being carbon. The isosurface is of the surface of constant spin density showing the localized nature of the orbital. The horizontal and vertical alignments are [110] and [001], respectively.

tive Si_s to V diminishes rapidly: 4.5, 1.6, 1.0, and less than 0.2 eV. Nevertheless, such complexes, once formed, would be stable at high T.

The Si atoms form Si-Si bonds, but the band gaps contain filled and empty orbitals, as indicated in Fig. 8. In the case of $(Si_s)_4$-V, the reconstruction is in pairs, yielding D_{2d} symmetry. The presence of gap levels renders these complexes electrically active with calculated acceptor levels at $E_v+2.4$ eV, $E_v+2.5$ eV, and $E_v+2.8$ eV for $n=2$, 3, and 4, respectively, and donor levels at $E_v+0.6$ eV and $E_v+1.4$ eV for $n=3$ and 4. The gap states also suggest that these complexes would be optically active, with transition energies, as determined crudely from the Kohn-Sham levels, in the region of 1.5–2.5 eV.

Finally, we note that the volume displaced by Si_s-V is around a third that of Si_s,[32,35] and therefore, these centers would lead to a proportionately smaller change in the lattice constant.

F. Vacancy-silicon-nitrogen complexes

As with Si_s, we have examined the propensity for Si_s-V to complex with nitrogen.

The substitution of C neighboring Si by nitrogen is highly advantageous for one or two sites, since this fully occupies the gap levels of Si_s-V and places nitrogen in a trivalent environment. This is reflected in the large binding energies. The addition of the first and second N atoms release 4.6 eV in both cases. However, additional N_s are only modestly bound (around 1.6 eV per N atom), since these centers are stabilized by the formation of broken N-C bonds containing the N_s donor electron.

Since the simultaneous incorporation of several nitrogen atoms at Si_s-V is unlikely during growth, the most probable structure in as-grown films is Si_s-V-$(N_s)_1$. The neutral charge state is EPR active, for which the calculated hyperfine tensors are listed in Table II. The lowering in symmetry due to the presence of the N atom localizes the unpaired electron on four of the five neighboring carbon atoms, as indicated in Fig. 9.

G. Silicon-hydrogen complexes

Given the suggestion that the KUL3 EPR center involves both Si and H, we have investigated Si_s-H and Si_s-V-H complexes.

TABLE II. Calculated hyperfine tensors (MHz) for Si_s-V-N_s in diamond. The angles in parentheses list deviations from indicated directions. The various carbon species are as labeled in Fig. 9.

Species	$\lvert A_1\rvert$	$\vec{A}_1$		$\lvert A_2\rvert$	$\vec{A}_2$		$\lvert A_3\rvert$	$\vec{A}_3$	
^{29}Si	92	[2 2 1]	(0°)	95	[$\bar{1}$ $\bar{1}$ 4]	(0°)	97	[$\bar{1}$ 1 0]	(0°)
^{1}N	0	[1 1 $\bar{1}$]	(3°)	−6	[1 1 2]	(3°)	−6	[$\bar{1}$ 1 0]	(0°)
$^{13}C_1$	77	[$\bar{1}$ 1 1]	(3°)	17	[2 1 1]	(4°)	16	[0 1 $\bar{1}$]	(4°)
$^{13}C_2$	4	[$\bar{1}$ $\bar{1}$ 1]	(3°)	−3	[1 1 2]	(3°)	−2	[$\bar{1}$ 1 0]	(0°)
$^{13}C_3$	65	[$\bar{1}$ 1 1]	(3°)	14	[$\bar{1}$ $\bar{2}$ 1]	(6°)	14	[1 0 1]	(6°)

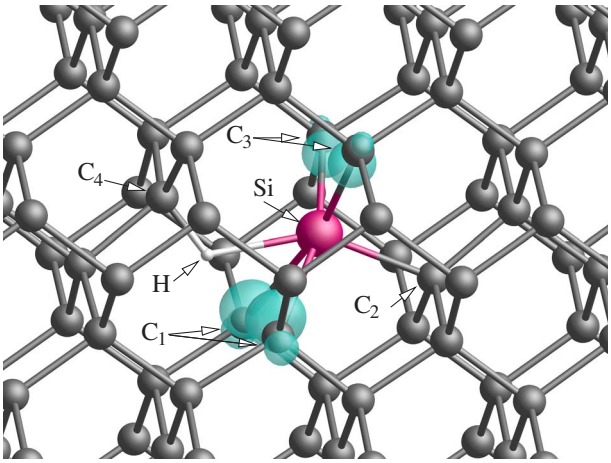

FIG. 10. (Color online) Schematic of the unpaired Kohn-Sham function for Si_s-V-H. Impurity atoms are as labeled, with all the remaining atoms being carbon. The isosurface is of the surface of constant spin density showing the localized nature of the orbital. The horizontal and vertical alignments are [110] and [001], respectively.

When H is in the immediate vicinity of Si_s, it has the lowest energy when bonded directly to the Si in an antibonding site along ⟨111⟩. This is in line with the calculated properties of H in the vicinity of other large substitutional impurities.[68] H in the bond center or antibonded to an adjacent C atom are 2.5 and 0.7 eV higher in energy, respectively. However, Si_s-H is unbound relative to isolated Si_s and H_i by around 0.4 eV. Given that H is predicted to be mobile at growth temperatures,[69] it seems unlikely that Si_s-H complexes would be present in an as-grown material.

It seems much more likely that H would bond in the vicinity of Si_s-V. Indeed, we find that Si_s-V-H is bound by 4.5 eV relative to Si_s-V and interstitial H. The complex is electrically active, with an acceptor level at $E_v+1.1$ eV, but in the neutral charge state, the complex is EPR active with a single unpaired spin. In addition, it has planar symmetry, as indicated in Fig. 10, so that the symmetry and effective spins agree with the KUL3 EPR center.[30] The calculated hyperfine tensors for this complex are listed in Table III. The H-related terms are in tolerable agreement with those of KUL3, which has published values[30] of around −3, 0, and 7 MHz. Additionally, the experimental orientation of 15° to a [110] direction in the $(10\bar{1})$ plane of the defect matches reasonably to a calculated value of around 10°.

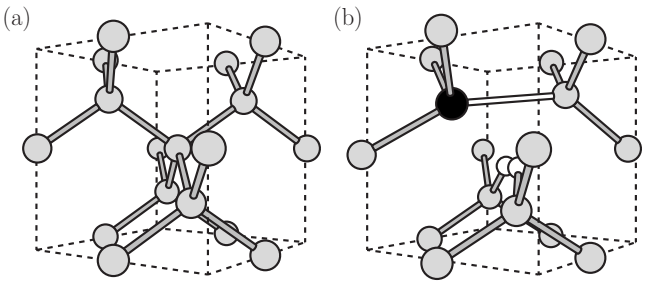

FIG. 11. Schematics of (b) Si_s-V-H_2 in diamond. The black, gray, and white atoms represent Si, C, and H, respectively. (a) shows the corresponding section of the bulk material for comparison.

The addition of a second hydrogen atom, which is bound by another 4.5 eV, largely passivates the complex, but there remains a potential acceptor level high in the band gap (E_c −0.5 eV). Thus, Si_s-V-H_2 may compensate shallow donors. Si_s-V-H_2 resembles Si_s neighboring V-H_2, with the Si atom forming a reconstruction with a C atom, as illustrated in Fig. 11.

Finally, we report the local vibrational modes of Si_s-V-H and Si_s-V-H_2. For Si_s-V-H, there is a single C-H (C-D) stretch mode at 3092 (2270) cm^{-1}. A bend mode lies at 1740 (1408) cm^{-1}. There is a Si-related mode calculated at around 320 cm^{-1} which also involves the motion H but shifting by just 3 cm^{-1} upon deuterium or ^{29}Si substitution. For the dihydride complex, there are odd and even combinations of C-H stretch modes, split by 240 cm^{-1} about a mean frequency of 3360 cm^{-1}. Odd and even combination of bend modes are also found at 1520 and 1400 cm^{-1}. A single mode at around 370 cm^{-1} is found where motion of the Si atom is significant. This mode shifts by around 5 and 10 cm^{-1} with ^{29}Si and ^{30}Si, respectively.

IV. DISCUSSION AND CONCLUDING REMARKS

The examination of a wide range of silicon-containing defect systems in diamond yields several specific results.

Individual interstitial silicon species are unstable at the growth temperature and possess a prohibitively high forma-

TABLE III. Calculated hyperfine tensors (MHz) for Si_s-V-H in diamond. The angles in parentheses list deviations from indicated directions. Carbon sites are indicated in Fig. 10.

Species	$\lvert A_1\rvert$	$\vec{A}_1$		$\lvert A_2\rvert$	$\vec{A}_2$		$\lvert A_3\rvert$	$\vec{A}_3$	
^{29}Si	86	$[\bar{1}\ \bar{1}\ 2]$	(3°)	88	$[\bar{1}\ \bar{1}\ \bar{1}]$	(3°)	89	$[\bar{1}\ 1\ 0]$	(0°)
^{15}H	−7	[2 2 3]	(2°)	3	$[\bar{2}\ \bar{2}\ 3]$	(2°)	6	$[\bar{1}\ 1\ 0]$	(0°)
$^{13}C_1$	16	$[\bar{2}\ \bar{1}\ \bar{1}]$	(2°)	90	$[1\ \bar{1}\ \bar{1}]$	(4°)	16	$[0\ 1\ \bar{1}]$	(4°)
$^{13}C_2$	−3	$[\bar{1}\ \bar{1}\ \bar{2}]$	(1°)	0	$[1\ 1\ \bar{1}]$	(1°)	−2	$[\bar{1}\ 1\ 0]$	(0°)
$^{13}C_3$	5	$[\bar{1}\ 1\ \bar{2}]$	(3°)	41	$[1\ \bar{1}\ \bar{1}]$	(3°)	4	[1 1 0]	(1°)
$^{13}C_4$	−7	$[\bar{2}\ \bar{2}\ \bar{1}]$	(2°)	−6	$[1\ 1\ \bar{4}]$	(2°)	61	$[\bar{1}\ 1\ 0]$	(0°)

tion energy. Theory therefore implies that Si_i should not be present in an as-grown material.

Si_s-V exhibits an isotropic ^{29}Si hyperfine tensor in all stable, paramagnetic charge states, consistent with the unpaired electrons being localized on the neighboring carbon atoms. The observation of KUL1 and KUL8 with $S=1$ and $S=1/2$, respectively, may be explained by the neutral and a charge state of Si_s-V. If, indeed, KUL8 contains one more electron than KUL1, as suggested from experiment, KUL8 would correspond with $(Si_s\text{-}V)^-$. However, we have previously correlated this structure with the TLS for which, apparently, there is no correlation with the EPR center.[9]

In defense of the model of $(Si_s\text{-}V)^-$ for the TLS, the orbital degeneracies explain the doublets observed experimentally, and the calculated vibrational modes broadly agree with that measured around 515 cm^{-1}. Furthermore, $(Si_s\text{-}V)^-$ is a Jahn-Teller system which would be consistent with a distortion to C_2 symmetry seen in uniaxial stress. This is less obvious in the neutral charge state, since the spin-triplet ground state is not a Jahn-Teller system, and one would expect a trigonal symmetry, as observed for the $S=1$, KUL1 EPR center. If this assignment is correct, this implies that the experimental electrical transition[26,27] around 2 eV below E_c must be the second acceptor level. This would relate to the dependence on nitrogen content rather simply. For low [N], Si_s-V is neutral and TLS would be weak; as [N] increases, the concentration of $(Si_s\text{-}V)^-$ increases until $(Si_s\text{-}V)^{2-}$ starts to dominate, leading to a maximum in TLS.

Therefore, there is a reasonable case to assign the KUL1 EPR center to $(Si_s\text{-}V)^0$ and the TLS and KUL8 to $(Si_s\text{-}V)^-$. The apparent lack of experimental correlation would require investigation but may be related to the inhomogeneous distribution of Si in the samples. EPR examines the entire sample, whereas optical measurements examine only a region.

Experiment also indicates the presence of other Si-related optical centers which have a different thermal stability from the TLS.[9,15] Si_s-V_2 and $(Si_s)_n$-V complexes possess band-gap states and must be candidate structures. Of these, the orthorhombic $(Si_s)_2$-V complex also exhibits Si-Si vibrational modes.

Energetically, silicon is unlikely to aggregate unless codoped with another impurity, such as nitrogen, or complexed with V. $(Si_s)_n$-N_s complexes where $n<4$ are deep donors and will not lead to n-type conduction, and all complexes containing a lattice vacancy and a number of silicon atoms act as deep electron traps. The formation of Si_s-N_s complexes during growth may contribute to the dependence of the concentration of optical centers upon the amount of N_2 in the feed gas.[14]

Nitrogen is also energetically favored when attached to Si_s-V complexes, with Si_s-V-N_s and Si_s-V-$(N_s)_2$ being particularly low energy systems. The former would be optically and EPR active in the neutral charge state but exhibit very little hyperfine interaction with the N atom. However, the presence of both low-symmetry and ^{29}Si hyperfine interactions might be viewed as characteristics that enable identification from experiment. For materials grown in the presence of high concentrations of nitrogen, the formation of Si_s-V-N_s, and possibly Si_s-V-$(N_s)_2$, might also be a factor in the magnitude of TLS.

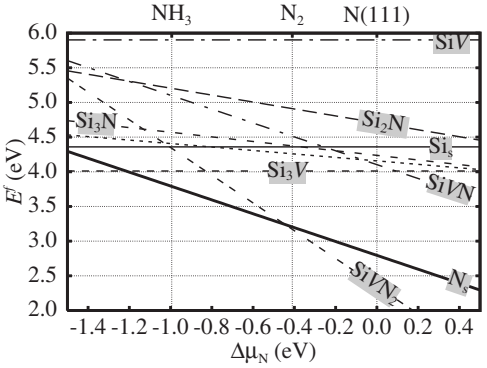

FIG. 12. E^f per Si atom for various Si and N containing defects in diamond. μ_{Si} and mu_C are taken from bulk materials. The unlabeled, dotted line corresponds to Si_4N. The zero of $\Delta\mu_N$ is taken from N on 1×1, N-terminated (111) surface, with locations for other N sources indicated at the top of the plot.

Similar to nitrogen, Si_s-V is a deep trap for hydrogen, and calculated hyperfine values for Si_s-V-H are in reasonable agreement with the KUL3 parameters.

Finally, we explore the energetics of the various complexes. The likelihood of a specific arrangement of constituents to combine to form a complex is related to the formation energy [Eq. (1)]. The difference in E^f between, for example, Si_4N and Si_s or Si_s-V-$(N_s)_n$ depends on the chemical potentials of N and Si. Figure 12 shows E^f for centers explored in this paper as a function of the μ_N. μ_{Si} is taken from bulk silicon, but because we plot E^f per Si atom, differences in formation energy are independent of this choice with the exception of N_s.

In Sec. III C, we showed that incomplete encapsulation of N_s by Si_s is competitive with Si_4N on energy grounds, but that these complexes are deep donors. The relative energy of $(Si_s)_3$-N_s to Si_4N is small over the range of μ_N, and one would expect these to form competitively, lowering the doping efficiency of Si_4N.

However, Fig. 12 indicates a more critical issue in this respect. In equilibrium, Si_s-V-$(N_s)_2$ is very stable, as would be expected for a system with its valence satisfied, and Si_s-V-$(N_s)_1$, an acceptor, is also relatively stable. In addition, Si_3-V, another acceptor, is the preferred structure for the incorporation of multiple Si impurities. At no point is Si_4N the preferred structure. Thermodynamically, there is no support for the formation of Si_4N in diamond. It is important to note that the current body of experimental evidence strongly indicates that formation of multi-impurity complexes during growth is uncommon. Even in a material with extremely high concentrations of boron, boron dimers are a small component, and although nitrogen dimers have been seen in as-grown diamond,[70] it is much more common for nitrogen to be incorporated as N_s or complexes with lattice vacancies. Therefore, the formation of complexes such as Si_3-V and Si_4N are unlikely unless there are specific mechanisms to incorporate these components simultaneously to form the complex structures. The most likely candidates must be

viewed as those such as Si_s-V, and possibly Si_s-V-$(N_s)_1$ or Si_s-V-H.

In the case of implantation, thermodynamics may give way to kinetics. Subsequent to implantation, the formation of acceptor complexes made up from Si_s and V are the most likely. We have shown that the binding energy of Si_s-V is very high, consistent with the thermal stability of the TLS. These deep acceptors may compensate n-type dopants.

Our final conclusion is therefore that Si-N codoping is unlikely to yield n-type conductivity from the formation of Si_4N complexes, with the uptake of Si more likely to lead to intrinsic material with deep donor and acceptor states in the band gap.

ACKNOWLEDGMENTS

We gratefully acknowledge M. E. Newton, P. M. Martineau, D. J. Twitchen, and A. M. Edmonds for discussion of recent unpublished experimental data. We also gratefully acknowledge the financial support of UK EPSRC.

[1] J. Barjon, E. Rzepka, F. Jomard, J.-M. Laroche, D. Ballutaud, T. Kociniewski, and J. Chevallier, Phys. Status Solidi A **202**, 2177 (2005).
[2] C. D. Clark, H. Kanda, I. Kiflawi, and G. Sittas, Phys. Rev. B **51**, 16681 (1995).
[3] C. L. Wang, C. Kurtsiefer, H. Weinfurter, and B. Burchard, J. Phys. B **39**, 37 (2006).
[4] C. D. Clark and C. B. Dickerson, Surf. Coat. Technol. **47**, 336 (1991).
[5] A. T. Collins, P. J. Woad, G. S. Woods, and H. Kanda, Diamond Relat. Mater. **2**, 136 (1993).
[6] G. Davies and M. H. Nazaré, J. Phys. C **13**, 4127 (1980).
[7] J. P. Goss, B. J. Coomer, R. Jones, T. D. Shaw, P. R. Briddon, M. Rayson, and S. Öberg, Phys. Rev. B **63**, 195208 (2001).
[8] H. E. Smith, G. Davies, M. E. Newton, and H. Kanda, Phys. Rev. B **69**, 045203 (2004).
[9] K. Iakoubovskii, A. Stesmans, M. Nesladek, and G. Knuyt, Phys. Status Solidi A **193**, 448 (2002).
[10] J. Ruan, W. J. Choyke, and W. D. Partlow, Appl. Phys. Lett. **58**, 295 (1991).
[11] T. Feng and B. D. Schwartx, J. Appl. Phys. **73**, 1415 (1993).
[12] A. T. Collins, M. Kamo, and Y. Sato, J. Mater. Res. **5**, 2507 (1990).
[13] M. Benabdesselam, P. Iacconi, J. E. Butler, and D. Briand, Diamond Relat. Mater. **10**, 2084 (2001).
[14] D. V. Musale, S. R. Sainkar, and S. T. Kshirsagar, Diamond Relat. Mater. **11**, 75 (2002).
[15] G. Sittas, H. Khanda, I. Kiflawi, and P. M. Spear, Diamond Relat. Mater. **5**, 866 (1996).
[16] I. Sakaguchi, M. N.-Gamo, K. P. Loh, H. Haneda, S. Hishita, and T. Ando, Appl. Phys. Lett. **71**, 629 (1997).
[17] L. Bergman, B. R. Stoner, K. F. Turner, J. T. Glass, and R. J. Nemanich, J. Appl. Phys. **73**, 3951 (1993).
[18] D. F. Talbot-Ponsonby, M. E. Newton, J. M. Baker, G. A. Scarsbrook, R. S. Sussmann, and C. J. H. Wort, J. Phys.: Condens. Matter **8**, 837 (1996).
[19] H. Sternschulte, K. Thonke, R. Sauer, P. C. Münzinger, and P. Michler, Phys. Rev. B **50**, 14554 (1994).
[20] A. V. Turukhin, C.-H. Liu, A. A. Gorokhovsky, R. R. Alfano, and W. Phillips, Phys. Rev. B **54**, 16448 (1996).
[21] A. A. Gorokhovsky, A. V. Turukhin, R. R. Alfano, and W. Philips, Appl. Phys. Lett. **66**, 43 (1995).
[22] S. W. Brown and S. C. Rand, J. Appl. Phys. **78**, 4069 (1995).
[23] A. M. Zaitsev, Phys. Rev. B **61**, 12909 (2000).
[24] I. Kiflawi, G. Sittas, H. Kandam, and D. Fisher, Diamond Relat. Mater. **6**, 146 (1997).
[25] K. Iakoubovskii, G. J. Adriaenssens, N. N. Dogadkin, and A. A. Shiryaev, Diamond Relat. Mater. **10**, 18 (2001).
[26] M. C. Rossi, S. Salvatori, and F. Galluzzi, Diamond Relat. Mater. **6**, 712 (1997).
[27] K. Iakoubovskii and G. J. Adriaenssens, Phys. Rev. B **61**, 10174 (2000).
[28] K. Iakoubovskii and A. Stesmans, Phys. Status Solidi A **186**, 199 (2001).
[29] K. Iakoubovskii and A. Stesmans, Phys. Rev. B **66**, 195207 (2002).
[30] K. Iakoubovskii, A. Stesmans, K. Suzuki, J. Kuwabara, and A. Sawabe, Diamond Relat. Mater. **12**, 511 (2003).
[31] Pan Bicai and Xia Shangda, Phys. Rev. B **49**, 11444 (1994).
[32] J. P. Goss, P. R. Briddon, M. J. Rayson, S. J. Sque, and R. Jones, Phys. Rev. B **72**, 035214 (2005).
[33] J. P. Goss, R. Jones, S. J. Breuer, P. R. Briddon, and S. Öberg, Mater. Sci. Forum **258-263**, 781 (1997).
[34] D. Segev and S.-H. Wei, Phys. Rev. Lett. **91**, 126406 (2003).
[35] J. P. Goss, P. R. Briddon, M. J. Rayson, S. J. Sque, and R. Jones, Phys. Rev. B **73**, 199904(E) (2006).
[36] J. P. Goss, R. Jones, S. J. Breuer, P. R. Briddon, and S. Öberg, Phys. Rev. Lett. **77**, 3041 (1996).
[37] J. P. Goss, P. R. Briddon, S. J. Sque, and R. Jones, Diamond Relat. Mater. **13**, 684 (2004).
[38] S. S. Moliver, Tech. Phys. **48**, 1449 (2003).
[39] J. P. Goss, P. R. Briddon, R. Sachdeva, R. Jones, and S. J. Sque, in *Physics of Semiconductors*, AIP Conf. Proc. Vol. 722A, edited by J. Menéndez and C. G. Van de Walle (AIP, Melville, NY, 2005), pp. 91–94.
[40] J. P. Goss, P. R. Briddon, and R. J. Eyre, Phys. Rev. B **74**, 245217 (2006).
[41] R. Jones and P. R. Briddon, in *Identification of Defects in Semiconductors*, Semiconductors and Semimetals Vol. 51A, edited by M. Stavola (Academic, Boston, 1998), Chap. 6.
[42] H. J. Monkhorst and J. D. Pack, Phys. Rev. B **13**, 5188 (1976).
[43] C. Hartwigsen, S. Goedecker, and J. Hutter, Phys. Rev. B **58**, 3641 (1998).
[44] J. P. Goss, M. J. Shaw, and P. R. Briddon, in *Theory of Defects in Semiconductors*, Topics in Applied Physics Vol. 104, edited by David A. Drabold and Stefan K. Estreicher (Springer, Berlin, 2007), pp. 69–94.
[45] D. A. Liberman, Phys. Rev. B **62**, 6851 (2000).
[46] G. Henkelman, B. P. Uberuaga, and H. Jónsson, J. Chem. Phys. **113**, 9901 (2000).

[47] G. Henkelman and H. Jónsson, J. Chem. Phys. **113**, 9978 (2000).
[48] S. B. Zhang and J. E. Northrup, Phys. Rev. Lett. **67**, 2339 (1991).
[49] G. Makov and M. C. Payne, Phys. Rev. B **51**, 4014 (1995).
[50] H. Nozaki and S. Itoh, Phys. Rev. E **62**, 1390 (2000).
[51] U. Gerstmann, P. Deák, R. Rurali, B. Aradi, Th. Frauenheim, and H. Overhof, Physica B **340-342**, 190 (2003).
[52] C. W. M. Castleton and S. Mirbt, Phys. Rev. B **70**, 195202 (2004).
[53] J. Shim, E.-K. Lee, Y. J. Lee, and R. M. Nieminen, Phys. Rev. B **71**, 035206 (2005).
[54] C. W. M. Castleton, A. Höglund, and S. Mirbt, Phys. Rev. B **73**, 035215 (2006).
[55] P. Erhart, K. Albe, and A. Klein, Phys. Rev. B **73**, 205203 (2006).
[56] M. J. Shaw, P. R. Briddon, J. P. Goss, M. J. Rayson, A. Kerridge, A. H. Harker, and A. M. Stoneham, Phys. Rev. Lett. **95**, 105502 (2005).
[57] P. E. Blöchl, Phys. Rev. B **50**, 17953 (1994).
[58] B. Hetényi, F. De Angelis, P. Giannozzi, and R. Car, J. Chem. Phys. **115**, 5791 (2001).
[59] J. P. Perdew, K. Burke, and M. Ernzerhof, Phys. Rev. Lett. **77**, 3865 (1996).
[60] P. Martineau (private communication).
[61] J. P. Goss, R. Jones, and P. R. Briddon, Phys. Rev. B **65**, 035203 (2002).
[62] J. P. Goss and P. R. Briddon, Phys. Rev. B **75**, 075202 (2007).
[63] D. J. Twitchen, M. E. Newton, J. M. Baker, T. R. Anthony, and W. F. Banholzer, Phys. Rev. B **59**, 12900 (1999).
[64] B. J. Coomer, A. Resende, J. P. Goss, R. Jones, S. Öberg, and P. R. Briddon, Physica B **273-274**, 520 (1999).
[65] H. Sternschulte, K. Thonke, J. Gerster, W. Limmer, R. Sauer, J. Spitzer, and P. C. Münzinger, Diamond Relat. Mater. **4**, 1189 (1995).
[66] G. Davies, S. C. Lawson, A. T. Collins, A. Mainwood, and S. J. Sharp, Phys. Rev. B **46**, 13157 (1992).
[67] R. Q. Hood, P. R. C. Kent, R. J. Needs, and P. R. Briddon, Phys. Rev. Lett. **91**, 076403 (2003).
[68] S. J. Sque, R. Jones, J. P. Goss, and P. R. Briddon, Phys. Rev. Lett. **92**, 017402 (2004).
[69] J. P. Goss, J. Phys.: Condens. Matter **15**, R551 (2003).
[70] K. M. McNamara, Appl. Phys. Lett. **83**, 1325 (2003).